JOURNAL OF CATALYSIS **162,** 209–219 (1996)
ARTICLE NO. 0278

The Origin of Sulfur Tolerance in Supported Platinum Catalysts: The Relationship between Structural and Catalytic Properties in Acidic and Alkaline Pt/LTL

J. T. Miller*,[1] and D. C. Koningsberger†

*Research and Development, AMOCO Oil Company, P.O. Box 3011, Mail Station H-9, Naperville, Illinois 60566-7011; and †Department of Inorganic Chemistry and Catalysis, Utrecht University, P.O. Box 80083, 3508 TB Utrecht, The Netherlands

Received November 10, 1995; revised April 22, 1996; accepted April 23, 1996

The reactivity, structure, and sulfur tolerance is compared for platinum supported on acidic and alkaline LTL zeolite. In the absence of sulfur, EXAFS spectroscopy indicates that small metallic platinum particles of approximately 6 to 14 atoms/cluster are present. The TOF for neopentane hydrogenolysis and isomerization is ca 100 times higher on the acidic LTL due to the metal–support interaction. Saturation of the platinum by H_2S, results in the formation of surface Pt–S bonds with a bond length of 2.33 Å. Comparison of the EXAFS results of the sulfur poisoned catalysts, indicates that the S to Pt ratio is lower for platinum on the acidic zeolite. Catalytically, the initial activity (per gram) of both catalysts is greatly reduced after sulfur poisoning due to the loss of exposed platinum, however, the initial neopentane TOFs are nearly unchanged. Because of its higher TOF, the catalytic activity (per gram) of sulfur poisoned, acidic Pt/LTL is comparable to that of nonsulfur poisoned alkaline Pt/LTL. In both sulfur poisoned catalysts the neopentane isomerization selectivity increases compared to the sulfur free catalyst. Although the initial TOFs of the nonsulfur poisoned and sulfur poisoned catalysts are the same, there is a rapid loss in activity due to coke formation in the sulfur poisoned, alkaline LTL, while rate of deactivation by coke in the sulfided, acidic LTL is much lower. The increased sulfur tolerance of acidic supported noble metal catalysts appears to result primarily from the higher intrinsic TOF. In addition, because of its resistance to coke deactivation, the acidic supported sulfur tolerant catalyst is able to maintain stable catalytic activity.

INTRODUCTION

Supported noble metal catalysts are used in a large number of commercially important applications, including hydrogenation, dehydrogenation, naptha reforming, isomerization, hydrocracking, oxidation, and automotive exhaust catalysts (1). While platinum is by far the most common catalytic metal, palladium, rhodium, iridium, and ruthenium are used in certain applications. Like all catalysts, supported metal catalysts are susceptible to poisoning by a variety of agents, one of the more common being sulfur. Several excellent reviews on sulfur poisoning of transition metal catalysts are available (2, 3). The susceptibility to poisoning by sulfur arises from the fact that there is a strong metal–sulfur chemisorption. Thus, even small amounts of sulfur present in the reactants can lead to saturation of the metal surface. The sensitivity to sulfur poisoning varies greatly with the particular application and catalyst. For example, Pt/LTL zeolite aromatization catalysts are extremely sensitive to sulfur poisoning, requiring feed sulfur levels below 0.05 ppm for adequate catalyst life (4, 5). In contrast, conventional Pt/alumina naphtha reforming catalysts operate with feed sulfur levels up to about 20 ppm (6–8), while bimetallic distillate aromatic saturation catalysts (PtPd/acidic zeolite) can tolerate up to 1000 ppm sulfur (9–12).

There is general agreement that noble metals supported on acidic supports are more sulfur tolerant than similar catalysts on non-acidic supports (9–20). For example, in the presence of 0.5 wt% thiophene, the steady state activity for o-xylene saturation by Pd in HY zeolite was many times higher than that for Pd in NaY. In addition, the sulfur tolerance decreased as the protons in Pd–HY were neutralized by Na^+ ions (15). Explanations for sulfur tolerance of acidic supported metal particles are most often ascribed to the electron deficient nature of the metal resulting from the interaction with the support (14, 15, 17–20). It is not clear, however, why electron deficient metal particles should be more sulfur tolerant. In one study, sulfur tolerance was observed to parallel the saturation sulfur coverage which decreased with increasing support acidity. The lower surface coverage was proposed to be due to the formation of weaker metal-sulfur bonds on acidic supports (17). Despite the general agreement that metal catalysts on acidic supports are more sulfur tolerant, a clear understanding of the effects of sulfur and the roles of various catalyst properties in improving sulfur tolerance is lacking.

In this study the structure and sulfur tolerance of platinum supported on acidic and alkaline LTL zeolite is

[1] Author to whom correspondence should be addressed.

0021-9517/96 $18.00

compared. The results indicate that there is a high surface coverage of sulfur in both catalysts with slightly less sulfur chemisorbed to Pt supported on acidic LTL. The sulfur tolerance of Pt/H-LTL results from its inherently higher TOF and the resistance to coke deactivation.

EXPERIMENTAL

Sample Preparation

The K-LTL zeolite (UOP) was converted into the NH_4^+ form by aqueous ion exchange with ten fold excess 1.5 M NH_4NO_3 at 60°C for 2 h. The zeolite was filtered, washed, and calcined at 540°C for 3 h. The elemental analysis for K-LTL were 14.0 and 8.3 wt% for K and Al, respectively (K/Al molar ratio of 1.16). The elemental analysis for H-LTL were 7.3 and 10.9 wt%, for K and Al (K/Al molar ratio of 0.46).

After zeolites had been calcined, the zeolite supports were impregated to 1.0 wt% Pt by contact with tetraammine platinum nitrate (Johnson Matthey) in H_2O. The resultant slurry was allowed to stand at room temperature for 3 h, after which it was dried at 120°C overnight. The crystallites of zeolite were held together without a binder. Ten grams of catalyst was reduced in 200 cc/min hydrogen by heating from room temperature to 250°C at 10°C/min. The catalyst was cooled in hydrogen and purged with N_2 at room temperature. Five grams of the reduced catalyst was again heated to 250°C in H_2. The H_2 was switched to H_2 with 500 ppm H_2S until H_2S was detected at the reactor outlet (ca 15 min) with lead acetate paper. The H_2S flow was continued for 30 min after which the flow was returned to H_2 for 30 min.

EXAFS

Data collection. The EXAFS measurements were made at the Synchrotron Radiation Source in Daresbury, UK, Wiggler Station 9.2, using a Si (220) double crystal monochromator. The storage ring was operated with an electron energy of 2 GeV and a current between 200 and 300 mA. At the Pt L_{III} edge (11564 eV), the estimated resolution was 3 eV. The monochromator was detuned to 50% intensity to avoid the effects of higher harmonics present in the X-ray beam. The measurements were done in the transmission mode. Data were collect in a *k*-scan mode with a 5-s data acquisition at 15 *k*.

Samples were pressed into a self-supporting wafers (calculated to have an absorbance of 2.5) and placed in a controlled atmosphere cell (21). The samples were reduced *in situ* at 250°C in flowing, prepurified, dry H_2 at 1 atm. Data were collected at liquid nitrogen temperature in the presence of H_2.

Data reduction. Standard procedures were used to extract the EXAFS data from the measured absorption spectra. The preedge background was approximated by a modified Victoreen curve (22), normalization was done by dividing the height of the absorption edge and the background was subtracted using cubic spline routines (23). The EXAFS data analysis was performed on the isolated part of the data obtained by an inverse Fourier transformation over a selected range in *r* space.

Reference data. Data for the phase shifts and backscattering amplitudes were obtained from EXAFS measurements of reference compounds (24). Pt foil was used for the Pt–Pt interactions, $Na_2Pt(OH)_6$ for the Pt–O interaction and H_2PtCl_6 for the Pt–S interactions.

Data analysis. To reliably determine the parameters characterizing the high Z (Pt) and low Z (O, S) contributions, multiple-shell fitting in *k*- and *r*-space was done, with application of k^1 and k^3 weighting. The use of both k^1 and k^3 weighting is a prerequisite since the *k*-dependence of the backscattering amplitude of the low Z elements is different fom the high Z elements. The backscattering amplitude of the low Z elements becomes very small above $k = 10$ Å^{-1}, in comparison with the amplitude of the high Z scatterers, which is still significant at higer values of *k* (25). Application of only k^3 weighting in systems containing both high and low Z scatters leads to underestimation of the low Z elements. In addition, optimizing k^1 and k^3 fits both in *k*- and in *r*-space results in a better decoupling of *N* (coordination number) and $\Delta\sigma^2$ (Debye–Waller factor) as well as *R* (coordination distance) and ΔE_0 (inner potential correction), and, therefore, leads to a more reliable set of parameters (24). Further optimization of the fit was done by applying the difference file technique and phase- and amplitude-corrected Fourier transforms (26).

The errors in the structural parameters were calculated from the covariance matrix taking into account the statistical noise of the EXAFS data and the correlations between the different coordination parameters. Systematic errors are not included in the calculation of standard deviations. The amplitude of the noise was estimated from the raw data at *k* values, where the EXAFS signal was sufficiently damped out. The values of the coodness of fit (ε_υ^2) were calculated as outlined in the Reports on Standards and Criteria in XAFS Spectroscopy (27).

Neopentane Hydrogenolysis/Isomerization

The conversion of neopentane was conducted at 400°C and atmospheric pressure in a fixed-bed reactor using 1.0 vol% neopentane in H_2. Catalyst powders were pressed into wafers and crushed to 42–80 mesh particles. The catalyst loadings were approximately 0.05 g diluted with 2g α-Al_2O_3 of the same particle size. For the most active catalyst, Pt/H-LTL, fine powders (less than 150 mesh) of catalyst and γ-Al_2O_3 (1 : 5 wt ratio) were well mixed, pressed into wafers, and crushed to 42–80 mesh. The catalysts were

prereduced at the reaction temperature for 1 h, and the conversion was adjusted from 0.5 to 2.0% by varying the space velocity. At each space velocity, the conversion was measured as a function of time. The initial conversion and selectivity were determine by extrapolation to time zero. The TOF (at time zero) was calculated based on the volumetric hydrogen and CO chemisorption and is reported as molecules/s/surface Pt atom. The selectivity is calculated on a molar basis as the percent of neopentane converted to isopentane (isomerization) and isobutane plus methane (hydrogenolysis) extrapolated to zero conversion and deactivation.

RESULTS

EXAFS Data Analysis

The EXAFS data (average of three scans) for Pt/H-LTL and Pt/K-LTL, with and without sulfur, are shown in Figs. 1a and 1b, respectively. The signal-to-noise ratio for the average data of Pt/H-LTL is 40 at 4 $Å^{-1}$, indicating that the data quality is sufficient to allow for a detailed EXAFS analysis. The EXAFS data for Pt/H-LTL in Fig. 1a (solid line) are characteristic for metallic platinum reduced at low temperature. The amplitude of the EXAFS between about $k = 2$ and 6 $Å^{-1}$ is influenced by low Z neighbors, for example oxygen ions from the support (28). The amplitude of the signal at high values of k is characteristic of metallic platinum. The dominating influence of sulfur in Pt(S)/H-LTL, Fig. 1a (dotted line), can clearly be seen from low k values up to about $k = 10$ $Å^{-1}$ with a beating node at ca 9.5 $Å^{-1}$. The characteristic features present in Fig. 1b are similar to those in Fig. 1a except that the amplitude of the Pt–Pt contribution is smaller in Pt/K-LTL than Pt/H-LTL; compare, for example, Figs. 1a and 1b (solid lines). The influence of sulfur is larger in Pt(S)/K-LTL than Pt(S)/H-LTL; compare Figs. 1a and 1b (dotted lines) for k values between about 2 and 6, for example.

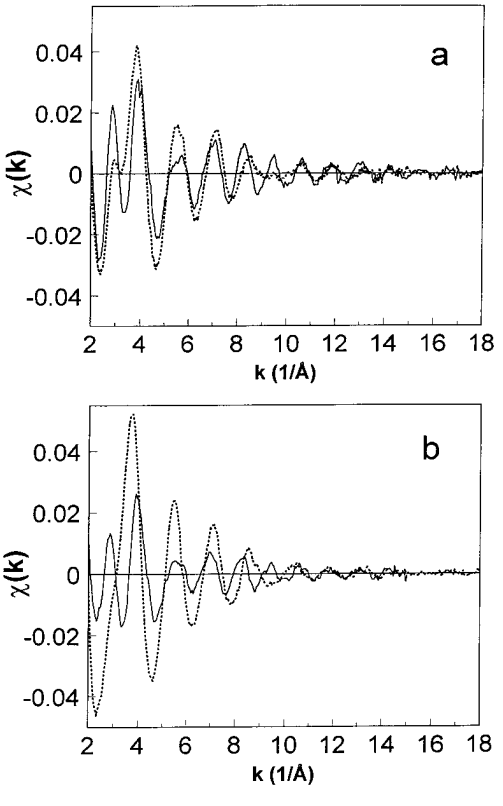

FIG. 1. EXAFS spectra of (a) Pt/H-LTL (solid line) and Pt(S)/H-LTL (dotted line), and (b) Pt/K-LTL (solid line) and Pt(S)/K-LTL (dotted line).

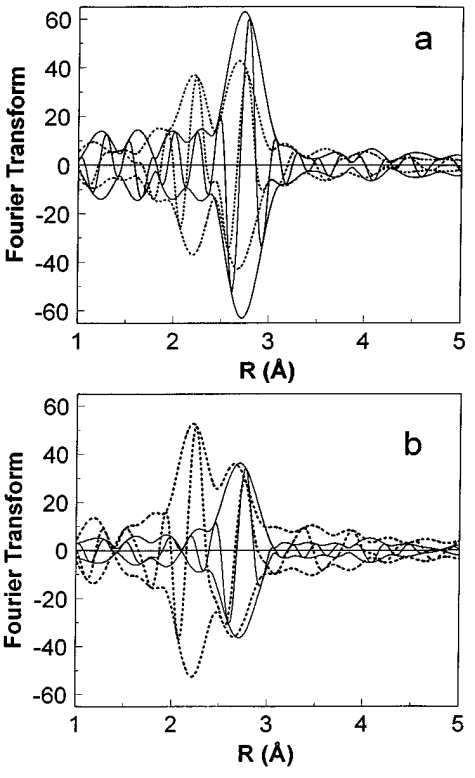

FIG. 2. Fourier transforms (k^3, $\Delta k = 3.2$–13.5 $Å^{-1}$, Pt–Pt phase and amplitude corrected) for (a) Pt/H-LTL (solid line) and Pt(S)/K-LTL (dotted line), and (b) Pt/K-LTL (solid line) and Pt(S)/K-LTL (dotted line).

The Fourier transforms (k^3, $\Delta k = 3.2$ to 13.5 $Å^{-1}$, Pt–Pt phase and amplitude corrected) of the catalysts with and without sulfur are presented in Fig. 2. The peak at around 2.7 Å is due the first coordination shell of metallic platinum and is present in all samples. Comparison of amplitudes of the Pt–Pt peak around 2.7 Å with and without sulfur indicates that for both catalysts the amplitude of the first shell platinum peak decreases on exposure to sulfur. In addition in the sulfur poisoned catalysts there is an additional scatterer at about 2.2 Å, which will be shown below to be due to the presence of sulfur.

The normalized k^1 weighted Fourier transform (Pt–Pt phase and amplitude corrected) of the EXAFS data for

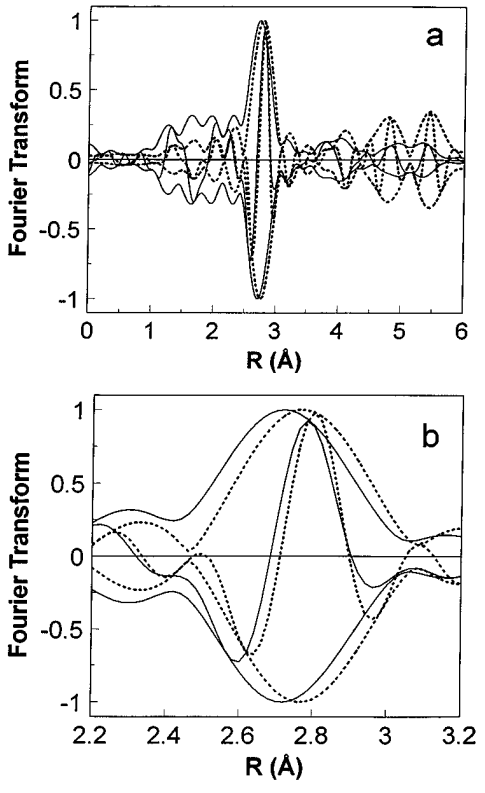

FIG. 3. Normalized Fourier transform (k^1, $\Delta k = 3.2$–13.5 Å^{-1}, Pt–Pt phase and amplitude corrected) for (a) Pt/H-LTL (solid line) and Pt foil (dotted line), and (b) an expanded view of 3a between $R = 2.2$–3.2 Å.

Pt/H-LTL and Pt foil are shown in Fig. 3. The Fourier transforms are normalized to facilitate comparison between the Pt foil and the catalyst. The near absence of higher Pt–Pt coordination shells (at 3.92, 4.80, and 5.54 Å) in the catalyst indicates that the platinum particles are small and reside within the zeolite pores (29). The particles are sufficiently small to detect contributions arising from the zeolite surface. Figure 3 is k^1 weighted in order to emphasize these low Z contributions, i.e., support oxygens. Evidence for this contribution can be seen more clearly in Fig. 3b which is an expansion of Fig. 3a from $r = 2.2$ to 3.2 Å. In Fig. 3b, the node position in the imaginary part of the Fourier transforms is identical for both the Pt foil and the catalyst at 2.9 Å. The node in the imaginary part for the catalyst around 2.7 Å, however, is shifted to lower R. Furthermore, the imaginary parts of the Fourier transforms between about 2.2 to 2.6 Å are completely different for the foil and the catalyst. These differences in the Fourier transforms indicate the presence of an additional oxygen scatter in the Pt/H-LTL catalyst (28).

Figure 4 shows a comparison of the Fourier transforms (Pt–Pt phase and amplitude corrected) for Pt(S)/H-LTL and Pt(S)/K-LTL catalysts. As discussed above, the peak around 2.2 Å (FT is not Pt–S phase corrected) is due to the Pt–S interaction and the peak around 2.7 Å is due to

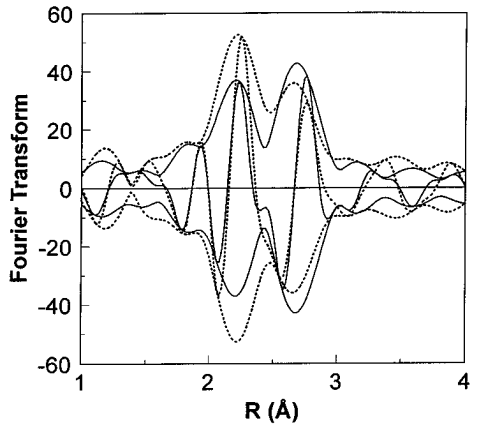

FIG. 4. Fourier transform (k^1, $\Delta k = 3.2$–13.5 Å^{-1}, Pt–Pt phase and amplitude corrected) for Pt(S)/H-LTL (solid line) and Pt(S)/K-LTL (dotted line).

the first shell Pt–Pt coordination. The peak characteristic for the Pt–S is larger in Pt(S)/K-LTL whereas the amplitude of the peak characteristic for Pt–Pt first shell coordination is slightly lower in Pt(S)/K-LTL. However, there is a strong overlap of the Pt–S and Pt–Pt peaks. As a result there is a contribution from the Pt–S beneath the Pt–Pt peak. Since the intensity of the Pt–S peak is larger in Pt(S)/K-LTL there is a larger Pt–S contribution to the Pt–Pt peak in this catalyst. Although the amplitude of the Pt–Pt peak in the Fourier transform of Pt(S)/K-LTL is only slightly smaller than that in Pt(S)/H-LTL, the larger contribution of the Pt–S in Pt(S)/K-LTL implies that the actual platinum particle size is smaller.

EXAFS Multiple Shell Fitting

Multiple shell fitting was conducted in k-space on Fourier filtered data. Fourier filtering was performed by forward Fourier transformation on k^2 (or k^3 for sulfided catalysts) weighted EXAFS data in order to minimize side lobes and peak widths resulting in a better separation of the EXAFS data from the background. The k range was selected to give the maximum range of reliable data with k_{min} and k_{max} taken at node positions (22). The inverse Fourier tranform range was selected to isolate the first shell coordination sphere of platinum. Because multiple electron excitations dominate the Fourier transform below about 1.5 Å, r_{min} was chosen at about this value. The ranges of Fourier filtering for each catalyst are listed in Table 1. The number of independent parameters allowed for the model fit was determined from these ranges according to the Nyquist theorem (27) and are also listed in Table 1.

The results of the multiple shell fitting in k-space (k^1 weighting) are given in Table 2. For both Pt/H-LTL and Pt/K-LTL the EXAFS can be fit with two significant contributions ($N_{fit} = 8$): a Pt–Pt coordination at 2.74 Å and a Pt–O coordination ca 2.7 Å. The goodness of fit values (0.7 and

TABLE 1

Fourier Filtering and Analysis Ranges of the EXAFS Model Fit[a]

Catalyst	k^n	Δk (Å^{-1})	ΔR (Å)	Δk_{anal} (Å^{-1})	N_{ind}[b]	υ[c]	Noise	ε_υ^{2}[d]
Pt/H-LTL	2	2.7–14.6	1.6–3.3	3.6–13.5	11.1	3.1	0.0015	0.7
Pt(S)/H-LTL	3	2.9–13.8	1.3–3.5	3.5–13.5	13.7	1.7	0.0015	0.4
Pt/K-LTL	2	2.6–14.0	1.6–3.3	3.6–13.0	11.2	3.2	0.0010	0.9
Pt(S)/K-LTL	3	2.0–13.6	1.4–3.3	3.2–13.5	13.7	1.7	0.0015	8.5

[a] All model fits used a k^1 weighting.
[b] N_{ind} is the number of independent fitting parameters, $N_{ind} = 2\Delta k \Delta R/\pi + 1$.
[c] υ is the degrees of freedom, $\upsilon = N_{ind} - N_{fit}$.
[d] ε_υ^2 is the goodness of fit, see the Report on Standards and Criteria (27).

0.9, for Pt/H-LTL and Pt/K-LTL, respectively) are given in Table 1. The quality of the fits is similar to those previously reported (28). For Pt/H-LTL, the Pt–Pt coordination number is 5.6 (ca 14 atoms/cluster), whereas the Pt–Pt coordination number is 4.0 (ca 6 atoms/cluster) for Pt/K-LTL. A long Pt–O distance around 2.7 Å is characteristic of platinum catalysts reduced at low temperature and is due to the presence of chemisorbed hydrogen between the metal cluster and the support surface (28, 30, 31). Because of the smaller platinum particle size in Pt/K-LTL, there is a larger Pt–O coordination number, e.g., $N = 0.9$ for Pt/K-LTL compared to $N = 0.5$ for Pt/H-LTL.

The results of the fit for Pt(S)/H-LTL in k- and r-space are presented in Fig. 5 with the coordination parameters given in Table 2. Similar quality fits were obtained for the other catalysts. For both Pt(S)/H-LTL and Pt(S)/K-LTL the EXAFS can be fit with three significant contributions ($N_{fit} = 12$): a Pt–Pt, a Pt–O, and a Pt–S coordination. The goodness of fit values are 0.4 for Pt(S)/H-LTL and 8.5 for Pt(S)/K-LTL (Table 1). For both Pt(S)/H-LTL and Pt(S)/K-LTL the Pt–Pt coordination number and distance decreases slightly compared to the sulfur free catalysts. For example, the Pt–Pt coordination distance decreases from 2.74 to 2.71 Å and the Pt–Pt coordination number decreases from 5.5 to 4.9 for the Pt/H-LTL catalysts after sulfur poisoning. The isolated Pt–S contribution for Pt(S)/H-LTL is given in Fig. 6a. The Pt–S phase corrected Fourier transform shows a Pt–S coordination distance at 2.33 Å. A similar Pt–S peak, but with increased amplitude, is observed for the

TABLE 2

EXAFS Model Coordination Parameters[a]

Backscatter Catalyst	N	R (Å)	$\Delta\sigma^2$ (Å^2)	ε_0 (eV)
Pt–Pt				
Pt/H-LTL	5.5 (4)	2.741 (4)	0.0028 (4)	5 (1)
Pt(S)/H-LTL	4.8 (8)	2.711 (5)	0.006 (1)	7 (1)
Pt/K-LTL	4.0 (3)	2.740 (6)	0.0042 (5)	5 (1)
Pt(S)/K-LTL	3.3 (6)	2.710 (9)	0.008 (1)	5 (1)
Pt–O				
Pt/H-LTL	0.7 (2)	2.66 (4)	0.004 (7)	1 (4)
Pt(S)/H-LTL	0.3 (1)	2.18 (9)	0.002 (10)	−7 (8)
Pt/K-LTL	0.9 (2)	2.70 (3)	0.008 (5)	−1 (3)
Pt(S)/K-LTL	0.5 (1)	2.20 (4)	0.001 (5)	−3 (4)
Pt–S				
Pt(S)/H-LTL	1.2 (2)	2.32 (1)	0.000 (1)	−3 (2)
Pt(S)/K-LTL	1.9 (2)	2.33 (1)	0.000 (1)	−1 (1)

[a] Values in brackets are the calculated limits of accuracy in the last reported digit.

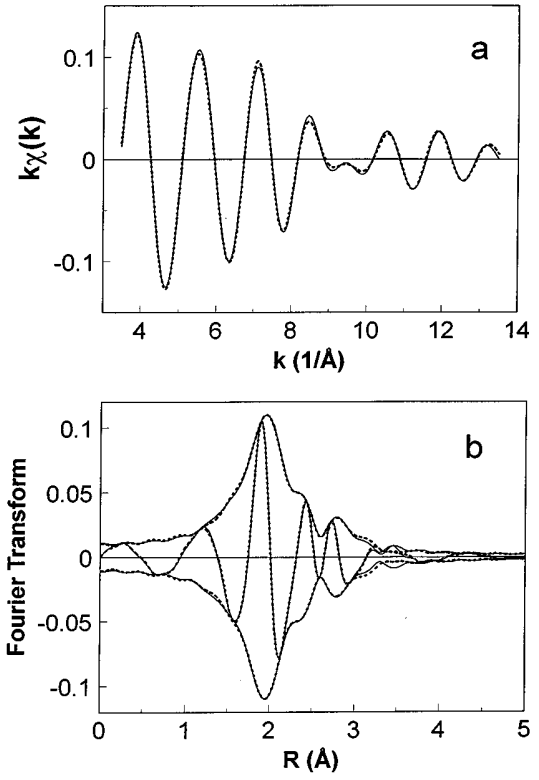

FIG. 5. Results of the EXAFS analysis for Pt(S)/H-LTL. (a) Isolated EXAFS (solid line) and the model EXAFS spectrum calculated from the parameters in Table 2 (dotted line), (b) Fourier transform (k^1, $\Delta k = 3.5$–13.5 Å^{-1}) of spectra in 5a.

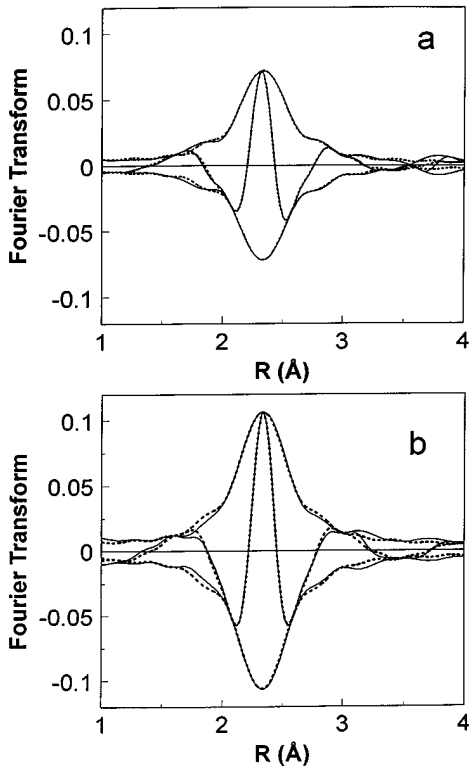

FIG. 6. The Fourier transform (k^1, $\Delta k = 3.5$–13.5 Å^{-1}, Pt–S phase corrected) of the (EXAFS data—(Pt–Pt + Pt–O contributions)) (solid line) and the model fit of the Pt–S contribution (dotted line) calculated from the parameters in Table 2. (a) Pt(S)/H-LTL and (b) Pt(S)/K-LTL.

Pt(S)/K-LTL catalyst, Fig. 6b. The Pt–O coordination distance for the sulfur poisoned catalysts is much smaller than that of the sulfur free catalysts. For example, in Pt/H-LTL the Pt–O coordination distance decreases from 2.66 to 2.18 Å upon exposure to sulfur. A Pt–O distance around 2.2 Å is characteristic of platinum atoms in direct contact with the support (28, 30, 31). The isolated Pt–O contributions for Pt/H-LTL and Pt(S)/H-LTL are given in Figs. 7a and 7b, respectively. The differences in peak positions can clearly be seen.

Catalytic Reaction of Neopentane

Analysis of the reaction products of neopentane at conversions between 0.5 and 2.0% by the Delplot method (32) indicate that methane, isobutane (hydrogenolysis), and isopentane (isomerization) are primary reaction products. For Pt/K-LTL and Pt(S)/H-LTL there was no deactivation; however, significant deactivation occurs for Pt/H-LTL and Pt(S)/K-LTL. For the latter two, the decrease in conversion with increasing time on stream was determined at constant space velocity. The ln(total conversion) versus time is linear and could be extrapolated to zero deactivation, i.e., zero time on stream, Fig. 8a. Similarly, the ln(selective conversion) for hydrogenolysis and isomerization versus time were linear, Fig. 8b. The selectivities were extrapolated to time zero to obtain the deactivation-free selectivity at that conversion. For example, in Fig. 8 the initial conversion is 1.49%, and the initial isomerization selectivity is 0.42. For Pt/H-LTL and Pt(S)/K-LTL, the initial conversion (zero time on stream) and selectivities were determined at several conversion levels. These initial conversions and selectivities were extrapolated to zero conversion to obtain the selectivity at zero conversion and zero deactivation. These initial catalyst selectivities and deactivation-free TOFs are given in Table 3.

As previously observed (30, 32, 33), the TOF for neopentane conversion by Pt/H-LTL is much higher, approximately 150 times, based on CO chemisorption (90 times higher, based on H_2 chemisorption) than that of Pt/K-LTL. In addition, the isomerization selectivity of Pt/K-LTL is 0.39, slightly higher than that of Pt/H-LTL, 0.35.

Poisoning of Pt/K-LTL by sulfur results in a large decrease in the absolute activity per gram of catalyst. The relative activity (per gram) of Pt(S)/K-LTL compared to Pt/K-LTL (defined to have a relative activity of 1.0) is also given in Table 3. Sulfur poisoning leads to a relative activity of 0.09 for Pt(S)/K-LTL. By contrast, the TOF of Pt(S)/K-LTL is not very different from that of Pt/K-LTL,

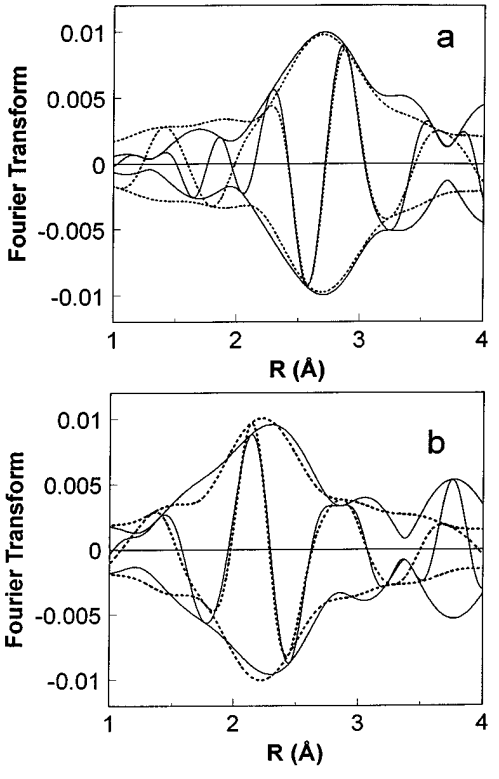

FIG. 7. The Fourier transform (k^1, $\Delta k = 3.5$–13.5 Å^{-1} Pt–O phase corrected) of the (EXAFS data—(Pt–Pt + Pt–S contributions)) (solid line) and the model fit of the Pt–O contribution (dotted line) calculated from the parameters in Table 2. (a) Pt/H-LTL and (b) Pt(S)/H-LTL.

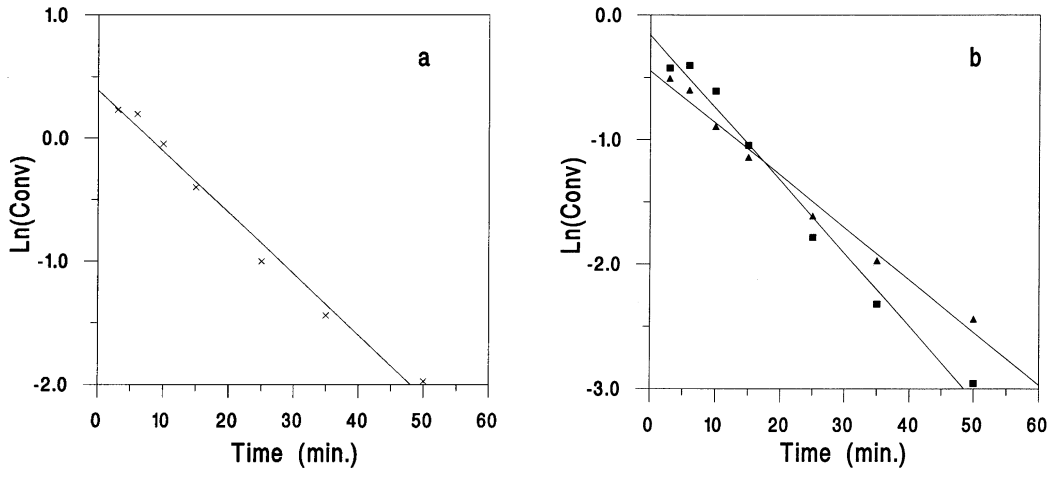

FIG. 8. Catalyst deactivation of neopentane (1% neopentane in H_2, atmospheric pressure, 400°C) for Pt(S)/K-LTL. (a) Total conversion (×), and (b) hydrogenolysis (square), and isomerization (triangle). Solid lines are model fits to data ($Conv_t = Conv_0 * e^{-kt}$).

about 0.01 molecules/s/surface Pt. The loss in activity due to sulfur poisoning, therefore, primarily results from the physical blockage of the platinum surface. As observed with other sulfur poisoned metal catalysts (6, 8, 35, 36), the hydrogenolysis selectivity decreases from 0.61 in Pt/K-LTL to 0.48 in Pt(S)/K-LTL, or the isomerization selectivity increases from 0.39 to 0.52.

Sulfur poisoning of Pt/H-LTL also leads to a large decrease in activity per gram of catalytst. For example, the relative activity/gram in Pt/H-LTL is 55 times higher than that in Pt/K-LTL, and decreases to 2 times higher in Pt(S)/H-LTL. It should be noted that the activity per gram of the sulfur poisoned Pt/H-LTL is still higher than the activity sulfur-free Pt/K-LTL (relative activity of 1.0). As observed for Pt(S)/K-LTL, the TOF is nearly the same as the sulfur-free catalysts, and the isomerization selectivity increases from 0.35 in Pt/H-LT to 0.80 in Pt(S)/H-LTL.

Also given in Table 3 are the deactivation rate constants based on the equation

$$Conv_t = Conv_0 * e^{-kt}$$

In the equation, Conv is the total neopentane conversion ($Conv_t$ = conversion at time on stream, $Conv_0$ = conversion at zero time on stream) and k is the deactivation rate constant with time measured in minutes. The space velocity was adjusted to give an initial conversion of 1% for each catalyst. The deactivation rate for each catalyst is shown in Fig. 9. As discussed above, the deactivation of Pt/H-LTL is much higher than Pt/K-LTL. Upon poisoning of Pt/K-LTL by sulfur, the deactivation rate constant increases from 6×10^{-4} to 5×10^{-2} min^{-1}, an increase of about 100 times. In Pt(S)/H-LTL, however, there is almost no deactivation, while there is a rapid loss in activity for sulfur free Pt/H-LTL.

DISCUSSION

Structural Characterization

The EXAFS analysis shows that for both the Pt/H-LTL and the Pt/K-LTL small platinum clusters are present. From the Pt–Pt coordination numbers, the number of platinum atoms/cluster can be estimated to be about 5 to 7 atoms for

TABLE 3

Activity, Selectivity and Deactivation Rate for Neopentane Hydrogenolysis[a]

Catalyst	Relative activity (per g catalyst)	TOF (H_2)	TOF (CO)	Isomerization selectivity[b]	Deactivation rate constant (min^{-1})
Pt/H-LTL (0.46)	55	0.9	1.5	0.35	2×10^{-2}
Pt(S)/H-LTL	1.8	2.5	2.1	0.80	6×10^{-4}
Pt/K-LTL (1.19)	1.0[c]	0.01	0.01	0.39	6×10^{-4}
Pt(S)/K-LTL	0.09	0.02	0.01	0.52	5×10^{-2}

[a] Determined at 400°C and 1 atm, 1% neopentane in H_2.
[b] Extrapolated to 0% conversion and deactivation.
[c] Defined to have a relative activity of 1.0/g catalyst.

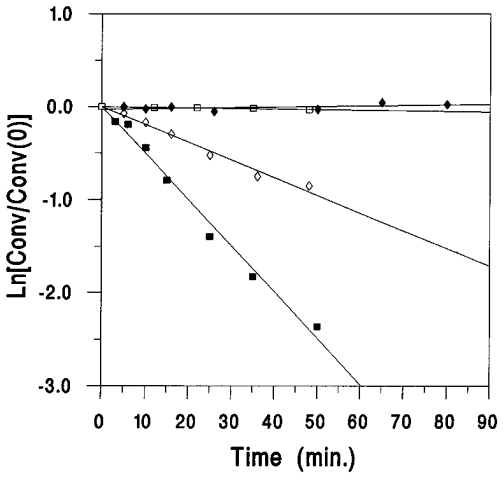

FIG. 9. Catalyst deactivation in the total conversion of neopentane (1% neopentane in H_2, atmospheric pressure, 400°C) for Pt/H-LTL (open diamond), Pt/K-LTL (open square), Pt(S)/H-LTL (closed diamond) and Pt(S)/K-LTL (closed square). The solid lines are model fits to data ($Conv_t = Conv_0 * e^{-kt}$), and the initial conversions were 1%.

Pt/K-LTL and 12 to 15 for Pt/H-LTL. Catalysts with similar EXAFS Pt–Pt coordination numbers and prepared by the same procedure leads to platinum clusters within the pores as evidenced by electron microscopy (29, 37). The Pt–Pt bond distance in the metallic clusters is 2.74 Å, 0.03 Å smaller than in Pt foil. A decrease of the metal–metal coordination distance can be expected when going from bulk metal to very small metal particles since the electron density in small particles is more localized on the metal atom, effectively shielding the internuclear replusion (38, 39). In a vacumn, a decrease in the metal–metal bond distance of approximately 0.1 Å has been observed for small metal particles, e.g., Pt/γ-Al_2O_3 (40), Pt/Y (41), and Ir/γ-Al_2O_3 (42). By contrast, bulk-like coordination distances are observed for small metal particles covered by chemisorbed hydrogen (28, 29, 40, 42). Chemisorbed hydrogen withdraws electron density from the metal atom which increases the internuclear repulsions and results in an expansion of the metal–metal bond distance. For the sulfur-free catalysts of this study, the platinum particles are so small that the contraction in the bond distance is not fully compensated by the expansion induced by chemisorbed hydrogen.

Because of the small size of the platinum clusters in both catalysts, oxygen ions from the support can be detected. Since the platinum particles are smaller in Pt/K-LTL than Pt/H-LTL, there is a larger fraction of the platinum atoms in contact with the support which is consistant with the larger Pt–O coordination number, e.g., $N = 0.9$ for Pt/K-LTL compared to $N = 0.5$ for Pt/H-LTL. The observed Pt–O distance around 2.7 Å is characteristic of platinum catalysts reduced at low temperature and is longer than the sum of the atomic radii for platinum and oxygen. This long distance results from the presence of chemisorbed hydrogen between the metal cluster and the support surface (28, 30, 31).

Severe sulfur poisioning of zeolite supported platinum clusters does not destroy the metallic properties. For both Pt(S)/H-LTL and Pt(S)/K-LTL, the Pt–Pt bond distance is 2.71 Å characteristic of metallic Pt (2.77 Å) and much shorter than the Pt–Pt distance in bulk PtS (3.47 Å) or bulk PtS_2 (3.54 Å) (43). Similar Pt–Pt distances have been previously observed in sulfur poisoned Pt/Ba-KLTL (44) and PtNi/K-LTL (45). Sulfur is chemisorbed on the outer surface of the metallic platinum particle with a Pt–S distance of 2.32 Å. The Pt–S distance is similar to that in bulk PtS (2.31 Å), but shorter than that in PtS_2 (2.40 Å) (43). A similar Pt–S structure, i.e., surface adsorbed sulfur on metallic platinum particles, with the same bond distance of 2.3 Å was previously reported for Pt/Ba-KLTL sulfur poisoned at 500°C (44). Sulfur poisoning also results in a decrease in the Pt–Pt bond distance and coordination number and an increase in disorder, compared to the unsulfided catalysts. For example, a Pt–Pt distance of 2.71 Å is 0.03 Å shorter than that in the sulfur-free catalysts and 0.06 Å shorter than that in Pt foil. As discussed above, a contraction of the platinum bond distance is expected because of the small particle size. At the same time, chemisorption of both hydrogen and sulfur would be expected to increase the Pt–Pt bond distance. In the sulfur poisoned catalysts, the hydrogen chemisorption capacity is very low (approximately 5% of the sulfur-free catalyst) due to the blockage of the surface atoms by sulfur. As a result, the expansion of the metal bond distance associated with chemisorbed hydrogen is small. The effect of chemisorbed sulfur, therefore, is not sufficient to fully compensate for the contraction of the bond distance in these small, surface–sulfide metal particles.

Although the decrease in bond distance suggests there is an increase in the Pt–Pt bond strength, in these platinum particles the number of nearest neighbors is very much smaller than is the bulk. As a result, the cohesive energy per Pt atom is smaller than in the bulk (36), resulting in a larger disorder in the sulfur poisoned catalysts.

Sulfur poisoning also leads to a slight decrease in Pt–Pt coordination number. Although this could be interpreted as a decrease in the metal particle size, it is not likely that at the low sulfiding temperatures that the platinum particles would be disrupted and that individual atoms would diffuse across the catalyst surface to form new, smaller platinum clusters. It seems more likely that upon sulfidation there is a small reorientation of the atoms leading to a small alteration in the particle morphology. In such a model, the number of atoms per clusters is unchanged, but there is a decrease in the number of nearest neighbor platinum atoms. Previous studies of sulfur poisoning of Pt in LTL zeolite at 500°C indicated that platinum particles increased in size, filling the zeolite pores (44, 46). By contrast, formation of bimetallic PtNi particles in *K*-LTL were resistant to sintering

by sulfur (45). At the lower temperatures of this study (250°C), sulfur does not appear to lead to sintering of the Pt particles.

In addition to changes in the structure of the platinum particles, sulfur adsorption induces changes in the structure of the metal–support interface. For example, after sulfur poisoning the Pt–O distance is 2.2 Å, compared to 2.7 Å in the sulfur-free catalysts. This shorter distance is characteristic of zero-valent metal atoms in direct contact with the oxide of the support (28, 31) and is typically observed after high temperature reduction (24), or evacuation after low temperature reduction (42). Because sulfidation and reduction were conducted at low temperature, the change in the Pt–O distance cannot be explained by thermal desorption of interfacial hydrogen (28). The low hydrogen chemisorption capacity of the sulfur poisoned suggests that platinum atoms with sulfur neighbors are unable to chemisorb hydrogen. It is possible that platinum atoms in contact with support oxygen ions, which additionally chemisorb sulfur, are unable to stabilize interfacial hydrogen resulting in a short Pt–O distance in Pt(S)/H-LTL and Pt(S)/K-LTL.

The EXAFS structural analysis show that the metal–sulfide phase is identical in Pt(S)/H-LTL and Pt(S)/K-LTL, differing only in the metal particle size, sulfur coordination, etc. Despite the structural similarities there is significantly less sulfur per surface platinum atom in the acidic supported catalyst. Based on the Pt–S coordination numbers and the small metal particle size of these catalysts, the ratio of sulfur to platinum surface atoms is approximately one for Pt(S)/H-LTL and two for Pt(S)/K-LTL.

Catalytic Properties

As previously observed for benzene hydrogenation (47, 48), propane hydrogenolysis (34, 49), and hydrogenolysis and isomerization of neopentane (30, 33, 34, 50–52), the TOF for neopentane conversion is higher for platinum on acidic zeolite, i.e., Pt/H-LTL as compared to alkaline Pt/K-LTL. For similar Pd/LTL catalysts this rate enhancement was shown to be due to a change in the electronic properties of the Pd induced by the support. For example, the Pd X-ray photoelectron spectra (XPS) showed an increase in the 3d binding energy of 0.6 eV for Pd/H-LTL and a decrease in binding enegy of −0.8 eV for Pd/K-LTL, compared to Pd foil, indicating the acidic-supported Pd is electron-deficient and the alkaline-supported Pd is electron-rich, compared to Pd foil. Furthermore, these shifts in the XPS binding energies were correlated with the changes in the neopentane and propane hydrogenolysis TOFs, indicating that the differences in the electronic properties are responsible for the observed changes in the specific rates. Additional evidence for a change in the electronic properties on these Pd catalysts was obtained from infrared spectroscopy. For both linear and bridge bonded CO, there is a decrease in the vibrational frequency as the alkalinity of the support increases. At the same time, a decrease in the ratio of linear to bridge bonded CO occurs as the alkalinity of the support increases; this is also consistent with an increase in the electron density of Pd on alkaline LTL (50). Similar shifts to lower frequency in the infrared spectra of the linear and bridge bonded CO are observed for Pt/LTL, again indicating a modification of the metal electronic properties by the support. At the same time as observed for Pd, there is a continual shift from linear to bridge bonded CO as the alkalinity of the support increases. Furthermore, this decrease in the ratio of linear to bridge bonded CO correlates with the decrease in the specific rate for neopentane hydrogenolysis of Pt, indicating that these changes in electronic properties induced by the supports are responsible for theses changes in specific activity (54). From the studies above, we conclude that the much higher TOF of Pt/H-LTL is due to the electron defficient nature of Pt on acidic H-LTL.

The activity per gram of catalyst of both sulfur-poisoned catalysts is much lower, approximately 5–10%, than that of the sulfur-free catalyst. Because of the much higher intrinsic activity of the Pt/H-LTL, even after sulfur poisoning, the activity per gram of Pt(S)/H-LTL is still higher than that of sulfur-free Pt/K-LTL. Although there is a large decrease in the per gram activity, the TOF of the sulfur-poisoned catalysts is nearly identical to that of the sulfur-free catalysts. The small differences in TOF between the sulfur-free and sulfur-poisoned catalysts likely results from the error in the chemisorption determination for the sulfur-poisoned catalysts which are very low. Because the TOF of the sulfur-poisoned and sulfur-free catalysts are essentially identical, the effect of adsorbed sulfur is primarily due to physical blockage of the surface platinum atoms. This implies that chemisorption of sulfur is not changing the electronic properties of the metal particle.

In addition to a decrease in the activity (per gram) of the sulfur poisoned catalysts, there is an increase in the isomerization selectivity. A structure-sensitive reaction like hydrogenolysis requires a larger ensemble of platinum atoms than isomerization (55, 56). Because of the high surface coverage of platinum by sulfur in both Pt(S)/H-LTL and Pt(S)/K-LTL, it is likely that the remaining, active platinum atoms are more isolated than in the sulfur-free catalysts. The lower hydrogenolysis selectivity of the sulfur-poisoned catalysts is consistant with a smaller ensenble size in the sulfided metal particles. Lower hydrogenolysis selectivties have been observed for other sulfur poisoned catalysts (6, 8, 35, 36).

Although the structure of the platinum–sulfur phase and the large effect of sulfur on the decrease in activity is identical for both acidic and alkaline supported platinum, the rate of deactivation by coke is much lower in the Pt(S)/H-LTL than in Pt(S)/K-LTL. From the EXAFS it was shown that

the sulfur coverage is much higher in Pt(S)/K-LTL, perhaps, with most of the sulfur-free platinum atoms completely isolated from other sulfur-free platinum surface sites. We propose that these isolated sites are not capable of simultaneous reaction with neopentane and hydrogen. Thus, these hydrogen deficient sites rapidly coke. Although the initial specific activity of Pt(S)/K-LTL is identical to that of sulfur-free Pt/K-LTL, the former does not maintain this activity due to coke formation. In Pt(S)/H-LTL, the lower sulfur coverage results in larger platinum ensembles which provide enough hydrogen to prevent rapid deactivation.

The deactivation rate of Pt(S)/H-LTL is also lower than that in sulfur-free Pt/H-LTL. Generally, coke deactivation of platinum during the conversion of neopentane is thought to result from adsorption of olefin intermediates (isobutylene and isopentene) on support acid sites. Since olefins react rapidly with the strong Bronsted acid sites in zeolites at the reaction conditions, it is likely that the olefin intermediates form coke at support sites near, or perhaps adjacent to, the platinum particles. These coke deposits would eventually decrease the platinum availability, leading to a loss in activity. Because of the high sulfur coverage of platinum in Pt(S)/H-LTL, fewer active platinum atoms may be near support acid sites. Thus, the amount of coke formed near the platinum–sulfur clusters is low. More work, however, is required to fully understand the low deactivation rate of the sulfur poisoned acidic supported platinum. Regardless of the reason, the low deactivation rate in Pt(S)/H-LTL is essential for maintenance of the activity in sulfur tolerant noble metal catalysts.

CONCLUSION

On acidic LTL zeolite, the specific rate of platinum for neopentane hydrogenolysis and isomerization is nearly 100 times higher than that on alkaline LTL. This enhanced rate is due to the interaction of the metal particles with the acidic support producing electron deficient platinum. Both acidic and alkaline supported platinum catalysts irreversibly loose much of their (sulfur free) activity when exposed to sulfur. Exposure of the small metallic particles to H_2S, results in the formation of surface Pt–S bonds. Simultaneously, there is a decrease in the Pt–Pt bond distance, a loss of interfacial hydrogen and a slight change in the particle morphology. Because of the much higher specific activity of acidic supported platinum, even after sulfur poisoning the activity per gram is still higher than that of sulfur free, alkaline supported platinum. Despite the large loss in the per-gram activity of both sulfur poisoned catalysts, the intrinsic activity of the remaining surface platinum atoms in the sulfur poisoned clusters is identical to that in the sulfur-free platinum clusters. The primary effect of adsorbed sulfur is due to the loss of active sites by physical blockage. Although platinum on acidic and alkaline supported LTL zeolite both irreversibly adsorb sulfur, the sufrace coverage (S to Pt ratio) is lower in acidic supported catalyst. Because of the high suface coverage of Pt in alkaline LTL, the active sites are more nearly isolated and are rapidly deactivated by coke. Sulfur tolerance of noble metals on acidic supports, therefore, results from their higher specific rate and their resistance to coke deactivation.

REFERENCES

1. "Oil and Gas Journal Data Book", Penn Well, Tulsa, 1994.
2. Bartholomew, C. H., Agrawal, P. K., and Katzer, J. R., *Adv. Catal.* **31**, 135 (1982).
3. Barbier, J., Lamy-Pitara, E., Marecot, P., Boitiaux, J. P., Cosyns, J., and Verna, F., *Adv. Catal.* **37**, 279 (1990).
4. Buss, W. C., Field, L. A., and Robinson, L. C., U.S. Patent No. 4,456,526 (1984).
5. Hughes, T. R., Buss, W. C., Tamm, P. W., and Jacobson, R. L., *in* "Stud. in Surf. Sci. and Catal. 28, Proc. 7th Int. Zeolite Conf." (Y. Murakami, A. Iijima, and J. W. Ward, Eds.), p. 725, Elsevier Sci., Amsterdam, 1986.
6. Menon, P. G., and Prasad, J., "Proceedings, 6 Int. Cong. Catal." (G. C. Bond, P. B. Wells, and F. C. Tomkins, Eds.), Vol. 2, p. 1061 Chem. Soc., London, 1977.
7. Gates, B. C., Katzer, J. R., and Schuit, G. C. A., "Chemistry of Catalytic Processes," p. 190, McGraw-Hill, New York, 1979.
8. Bickle, G. M., Biswas, J., and Do, D. D., *Appl. Catal.* **36**, 259 (1988).
9. Minderhoud, J. K., and Lucien, J. P., European Patent No. 303,332, "A Process for Hydrogenation of Hydrocarbon Oils."
10. Kukes, S. G., Clark, F. T., and Hopkins, P. D., U.S. Patent No. 5,147,426, "Distillate Hydrogenation."
11. Kukes, S. G., Clark, F. T., Hopkins, P. D., and Green, L. M., U.S. Patent No. 5,151,172, "Distillate Hydrogenation."
12. van den Berg, J. P., Lucien, J. P., Germaine, G., and Thielemans, G. L. B., *Fuel Proc. Technol.* **35**, 119 (1993).
13. Rabo, J. A., Shomaker, V., and Pickert, P. E., *in* "Proceedings, 3rd Int. Cong. Catal." (W. M. H. Sachtler, G. C. A. Schuit, and P. Zwietering, Eds.), Vol. 2, p. 1264, North-Holland, Amsterdam, 1965.
14. Chukin, G. D., Landau, M. V., Kruglikov, V. Y., Agievskii, D. A., Smirnov, B. V., Belozerov, A. L., Asrieva, V. D., Goncharova, N. V., Radchenko, E. D., Konoval'chikov, O. D., and Agafonov, A. V., *in* "Proceedings, 6 Int. Cong. Catal." (G. C. Bond, P. B. Wells and F. C. Tomkins, Eds.), Vol. 2, p. 1264, Chem. Soc., London, 1977.
15. Landau, M. V., Kruglikov, V. Y., Goncharova, N. V., Konoval'chikov, O. D., Chukin, G. D., Smirnov, B. V., and Malevich, V. I., *Kinet. Catal.* **17**, 1104 (1976).
16. Kovach, S. M., and Kmecak, R. A., *Prepr. Am. Chem. Soc. Div. Pet. Chem.* **25**(1), 79 (1980).
17. Frety, R., Da Silva, P. N., and Guenin, M., *Catal. Lett.* **3**, 9 (1989).
18. Frety, R., Da Silva, P. N., and Guenin, M., *Appl. Catal.* **57**, 99 (1990).
19. Hoyos, L. J., Primet, M., and Praliaud, H., *J. Chem. Soc. Faraday Trans.* **88**, 113 (1992).
20. Marecot, P., Mahoungou, J. R., and Barbier, *Appl. Catal. A Gen.* **101**, 143 (1993).
21. Kampers, F. W. H., Mass, T. M. J., van Grondelle, J., Brinkgreve, P., and Koningsberger, D. C., *Rev. Sci. Instr.* **60**, 2645 (1989).
22. Vaarkamp, M., Dring, I., Oldman, R. J., Stern, E. A., Koningsberger, D. C., *Phys. Rev. B* **50**, 7872 (1994).
23. Cook, J. W., Jr., and Sayers, D. E., *J. Appl. Phys.* **52**, 5024 (1981).
24. Kampers, F. W. H., Engelen, C. W. R., Van Hooff, J. H. C., and Koningsberger, D. C., *J. Phys. Chem.* **94**, 8574 (1990).
25. Koningsberger, D. C., *in* "Physics and Chemistry of Solids. Hercules Course" (J. Baruchel, J. L. Houdeau, M. S. Lehmann, J. R. Regnard, and C. Schlenker, Eds.), Vol. II, p. 213, Springer-Verlag, Berlin, 1993.

26. Duivenvoorden, F. B. M., Koningsberger, D. C., Uh, Y. S., and Gates, B. C., *J. Am. Chem. Soc.* **108**, 6254 (1986).
27. Lytle, F. W., Sayers, D. E., and Stern, E. A., *Physica B* **158**, 701 (1989).
28. Vaarkamp, M., Modica, F. S., Miller, J. T., and Koningsberger, D. C., *J. Catal.* **144**, 611 (1993).
29. Miller, J. T., Sajkowski, D. J., Modica, F. S., Lane, G. S., Gates, B. C., Vaarkamp, M., Grondelle, J. V., and Koningsberger, D. C., *Catal. Lett.* **6**, 369 (1990).
30. Miller, J. T., Meyers, B. L., Modica, F. S., Lane, G. S., Vaarkamp, M., and Koningsberger, *J. Catal.* **143**, 395 (1993).
31. Koningsberger, D. C., Vaarkamp, M., Munoz Paez, A., and van Zon, F. B. M., *in* "X-ray Absorption Fine Structure (XAFS) for Catalysis and Surfaces" (Y. Iwasawa, Ed.), to be published.
32. Bhore, N. A., Klein, M. T., and Bischoff, *Ind. Eng. Chem. Res.* **29**, 313 (1990).
33. Modica, F. S., Miller, J. T., Meyers, B. L., and Koningsberger, D. C., *Catal. Today* **21**, 37 (1994).
34. Mojet, B. L., Kappers, M. J., Muijsers, J. C., Niemantsverdriet, J. W., Miller, J. T., Modica, F. S., and Koningsberger, D. C., *in* "Stud. in Surf. Sci. and Catal., 84B, Zeolites and Microporous Materials: State of the Art 1994" (J. Weitkamp, H.G. Karge, H. Pfeifer and W. Holderich, Eds.), p. 909, Elsevier Sci., Amsterdam, 1994.
35. Menon, P. G., Marin, G. B., and Froment, G. F., *Ind. Eng. Chem. Prod. Res. Dev.* **21**, 52 (1982).
36. Coughlin, R. W., Hasan, A., and Kawakami, K., *J. Catal.* **88**, 163 (1984).
37. Lane, G. S., Modica, F. S., and Miller, J. T., *J. Catal.* **129**, 145 (1991).
38. Delly, B., Ellis, D. E., Freeman, A. J., Baerends, E. J., and Post, D., *Prys. Rev. B* **27**, 2132 (1983).
39. Balerna, A., and Mobilio, S., *Prys. Rev. B* **34**, 2293 (1986).
40. Vaarkamp, M., thesis, "The Structure and Catalytic Properties of Supported Platinum Catalysts," Einhoven University of Technology, The Netherlands, 1993.
41. Moraweck, B., Glugnet, G., and Renouprez, A. J., *Surf. Sci.* **81**, L631 (1979).
42. Kampers, F. W. H., and Koningsberger, D. C., *Faraday Discuss. Chem. Soc.* **89**, 137 (1990).
43. Gronvold, F., Haraldsen, H., and Kjekshus, A., *Acta Chem. Scand.* **14**, 1879 (1960).
44. Vaarkamp, M., Miller, J. T., Modica, F. S., Lane, G. S., and Koningsberger, D. C., *J. Catal.* **138**, 675 (1992).
45. Larsen, G., Ressasco, D. E., Durante, V. A., Kim, J., and Haller, G. L., *in* "Stud. in Surf. Sci. and Catal., 83, Zeolites and Microporous Crystals" (T. Hattori, and T. Yashima, Eds.), p. 321, Kodansha, Toyko and Elsevier, Amsterdam, 1994.
46. McVicker, G. B., Kao, J. L., Ziemiak, J. J., Gates, W. E., Robbins, J. L., Treacy, M. M. J., Rice, S. B., Vanderspurt, T. H., Cross, V. R., and Ghosh, A. K., *J. Catal.* **139**, 48 (1993).
47. Figueras, F., Gomez, R., and Primet, M., *in* "Molecular Sieves," Adv. Chem. Ser. Vol. 121 (W. M. Meier and J. B. Uytterhoeven, Eds.), p. 480, ACS, Washington, DC, 1973.
48. Lin, S. D., and Vanice, M. A., *J. Catal.* **143**, 539 (1993).
49. Vaarkamp, M., Miller, J. T., Modica, F. S., Lane, G. S., and Koningsberger, D. C., *in* "Stud. in Surf. Sci. and Catal., 75A, New Frontiers in Catalysis" (L. Guczi, F. Solymosi, and P. Tetenyi, Eds.), p. 809, Elsevier, Amsterdam, 1993.
50. Hoymeyer, S. T., Karpinski, Z., and Sachtler, W. M. H., *J. Catal.* **123**, 60 (1990).
51. Karpinski, Z., Gandhi, S. N., and Sachtler, W. M. H., *J. Catal.* **141**, 337 (1993).
52. Larsen, G., and Haller, G. L., *Catal. Today* **15**, 431 (1992).
53. van Santen, R. A., *J. Chem. Soc. Faraday Trans. I* **83**, 1915 (1987).
54. Mojet, B. L., Kappers, M. J., Miller, J. T., and Koningsberger, D. C., *in* "Stud. in Surf. Sci. and Catal., 101, Procs. 11th Int. Cong. of Catal." (J. W. Hightower, W. N. Delgass, E. Iglesia, and A. T. Bell., Eds.), p. 1165, Elsevier, Amsterdam, 1996.
55. Frennet, A., Lienard, G., Crucq, A., and Degols, L., *J. Catal.* **53**, 150 (1978).
56. Boudart, M., and Dejega-Mariadassou, G., "Kinetics of Heterogeneous Catalytic Reactions" (J. M. Prausnitz and L. Brewer, Eds.), p. 173, Princeton Univ. Press, Princton, NJ, 1984.